

Figure S1

Figure S1: Floxed alleles of AMPK α 1 and α 2 escape Ad-Cre mediated recombination in Kras^{G12D} lung tumors, and AMPK loss does not phenocopy LKB1 loss in Kras^{G12D} dependent NSCLC, Related to Figure 1

(A) *Left:* Western blot for AMPK α 1 and AMPK α 2 protein expression in the indicated human NSCLC cell lines. *Right:* Western blot for AMPK α 1 and AMPK α 2 protein expression in Kras^{G12D} lung tumors.

(B) *Left:* P-ACC IHC in livers that are either proficient (+/+) or deleted (Alb-Cre/+) for AMPK α 1/ α 2.

Scale bar, 50 μ M. *Right:* P-ACC IHC in lung tumors of mice that were either control treated or treated with the ACC inhibitor ND-646. Scale bar, 50 μ m.

(C) Deletion of AMPK α 1 or AMPK α 2 alone does not eliminate P-ACC^{S79} staining; deletion of both AMPK α 1 and AMPK α 2 ("KA") is required to completely ablate P-ACC^{S79} staining. P-ACC IHC in lungs of Kras-WT (K), Kras-AMPK α 1^{F/F} (KA1), Kras-AMPK α 2^{F/F} (KA2) or Kras-AMPK α 1/ α 2^{F/F} (KA) mice.

Scale bar, 2000 μ m.

(D) To assess the impact of AMPK deletion on AMPK signaling in lung tumors, we plucked individual lung tumors from KA mice and immunoblotted for AMPK protein expression and phosphorylation of direct AMPK substrates. A number of KA tumors had significant expression of either or both AMPK α 1 and α 2 subunits and had also retained phosphorylation of AMPK substrates such as P-ACC^{S79} and P-Raptor^{S792}, suggesting that many 'KA' lung tumors had not efficiently deleted the α 1 and α 2 subunits of AMPK. Western blots on single primary K and KA tumor lysates. Number of tumors analyzed per genotype is shown.

(E) To determine whether KA lung tumors had escaped deletion, we assessed Cre-mediated recombination at the genomic DNA level. We generated primers specific for either the recombined or floxed alleles of AMPK α 1 and α 2 and then we performed laser capture micro-dissection (LCM) on single individual tumors from formalin fixed paraffin embedded (FFPE) lung sections, isolated genomic DNA (gDNA) and assessed AMPK α 1 and α 2 recombination by PCR. We found that several KA lung tumors had escaped recombination of AMPK α 1 and α 2, which explains the significant retention of AMPK protein expression observed in tumor lysates. We detected floxed alleles of AMPK α 1 and α 2 in all tumors analyzed, regardless of whether we also detected recombined AMPK, suggesting that either

recombination of AMPK is heterozygous in some tumors or that the presence of the floxed allele is from non-tumor tissue such as stromal cells or infiltrating immune cells. *Top*: Diagram depicting AMPK α 1 and AMPK α 2 genomic locus and design of primers to amplify the recombined allele of AMPK or the floxed allele. Expected PCR product sizes are shown. *Bottom*: PCR for recombined or floxed AMPK from genomic DNA isolated from single KA tumors by LCM. Number of tumors analyzed is shown.

(F) Schematic of experimental design in Kras (K), Kras-AMPK α 1 (KA1), Kras-AMPK α 2 (KA2), Kras-AMPK α 1/ α 2 (KA) and Kras-LKB1 (KL) floxed mouse models administered Ad-Cre.

(G) Fold change in BLI during the imaging period.

(H) Longitudinal BLI data from Ad-Cre induced tumors. Average BLI is plotted.

(I) Representative overlay images from bioluminescence imaging (BLI). Scale bar represents photons/sec/cm²/sr.

(J) *Left*: P-ACC IHC in KA mice. *Right*: P-AMPK IHC in a serial section. An example of an escaper tumor and an AMPK deleted tumor is shown. Scale bar, 5000 μ m.

(K) P-ACC IHC in lungs of K and KA mice induced with either Ad-Cre (*left*) or Lenti-Cre (*right*). Scale bar, 2000 μ m.

(L-N) Post hoc analyses from H&E sections. KA tumors that escaped deletion of AMPK were identified by P-ACC IHC analysis of serial sections to those stained with H&E and excluded from the data shown.

(L) Tumor burden analysis in Ad-Cre induced tumors. Tumor area was calculated as a percentage of total lung area per mouse.

(M) Average tumor number per mouse in Ad-Cre induced tumors.

(N) Tumor size (area in mm²) in Ad-Cre induced tumors. Each dot represents a single tumor.

(O-P) Average tumor number (O) and average tumor area (P) per mouse in K, KA1 or KA2 mice.

(Q) P-ACC IHC in lungs of K and KL mice.

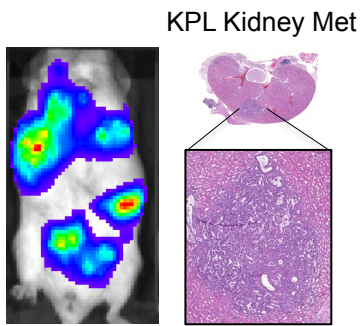
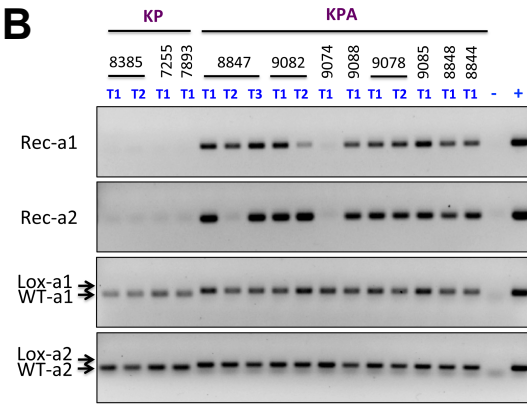
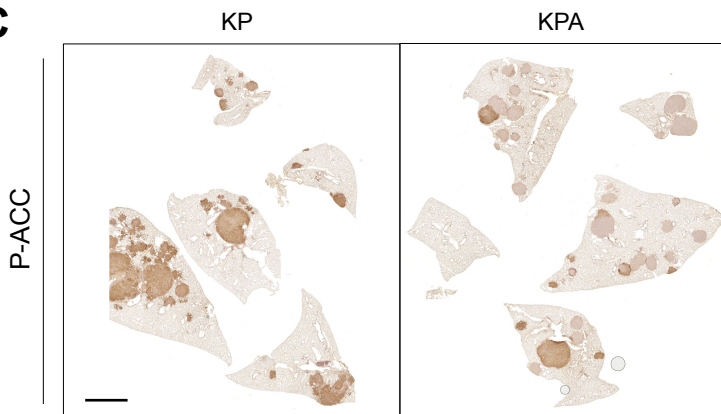
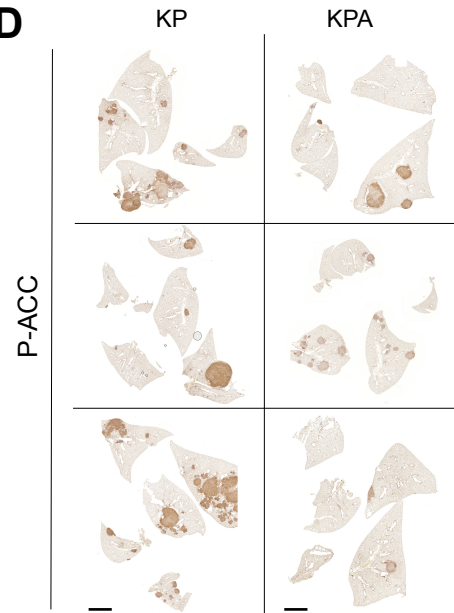
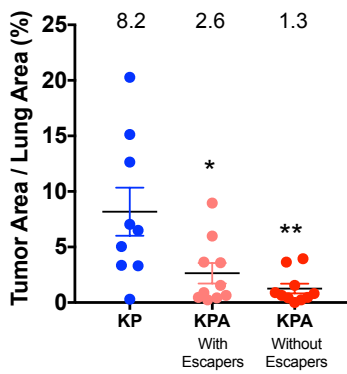
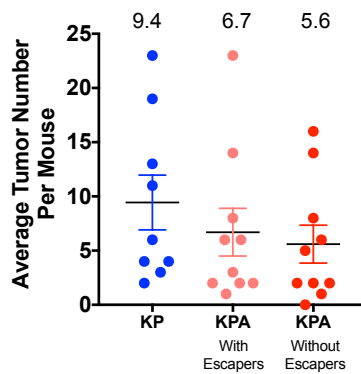
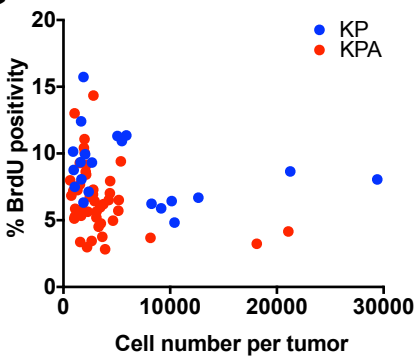
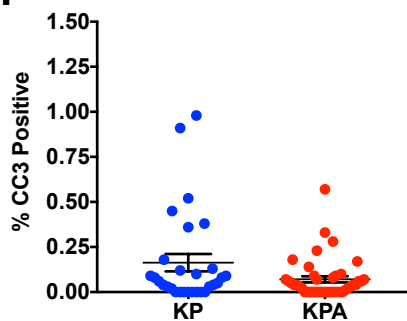
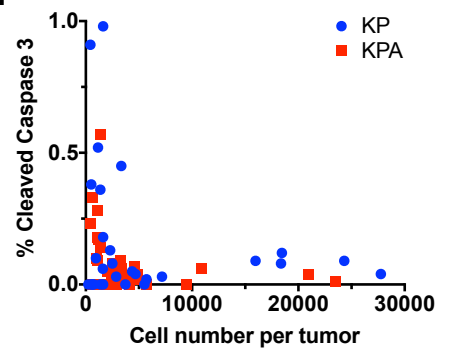
A**B****C****D****E****F****G****H****I**

Figure S2: AMPK deletion is detrimental to the growth of $Kras^{G12D}$ $p53^{-/-}$ (KP) NSCLC, Related to Figure 2

(A) Bioluminescence overlay image from a KPL mouse depicting metastatic lesions outside of the thoracic cavity. H&E image shows a metastatic tumor in the kidney.

(B) PCR for the recombined or floxed allele of AMPK from genomic DNA isolated from single KP and KPA tumors. Numbers indicate mouse ID and number of tumors analyzed per mouse.

(C) P-ACC IHC images in KP and KPA mice. Scale bar, 2000 μ m.

(D) P-ACC IHC images in KP and KPA mice.

(E) Tumor burden analysis. Tumor area was calculated as a percentage of total lung area. Each dot represents the average tumor burden of a single mouse. The mean is written at top.

(F) Average tumor number per mouse. Each dot represents an individual mouse. The mean is written at top.

(G) % BrdU positivity plotted by tumor size. Each dot represents an individual tumor.

(H-I) Quantitation of Cleaved Caspase 3 (CC3) positivity in KP and KPA tumors (H) and quantitation of CC3 positivity plotted by tumor size for each genotype (I). Each dot represents an individual tumor.

All values are expressed as means \pm s.e.m. * $P < 0.05$ ** $P < 0.01$ *** $P < 0.001$ relative to KP determined by students t test.

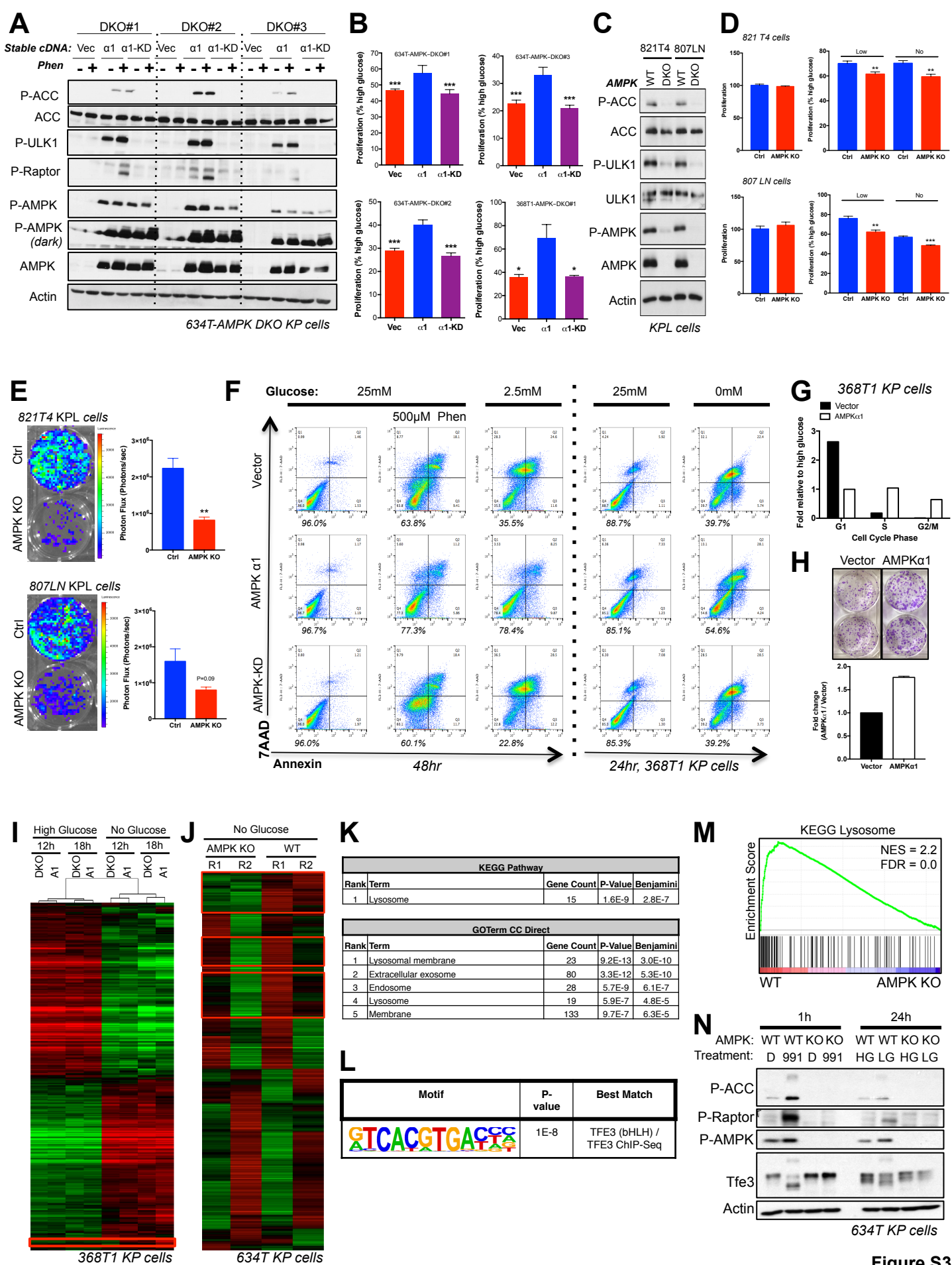


Figure S3

**Figure S3: AMPK promotes lysosomal gene expression upon glucose starvation in NSCLC cells,
Related to Figure 3**

(A) Western blot of KP 634T AMPK DKO isogenic clones left untreated or treated with 2mM phenformin for 1hr.

(B) Proliferation rates of 634T AMPK DKO isogenic cell lines in low glucose after 48hrs. Data are represented as percent proliferation of cells in high glucose.

(C) Western blot of KPL cell lines 821T4 and 807LN stably infected with Lentiviral-mediated CRISPR/Cas9 inactivation of control (WT) or AMPK α 1 and α 2 (DKO) in a pooled cell population.

(D) Proliferation rates of WT (Ctrl) or AMPK KO KPL cell lines in low glucose after 48hrs. Data are represented as percent proliferation of cells in high glucose.

(E) Growth in soft agar of 821T4 and 807LN cells stably expressing luciferase then stably infected with Lentiviral-mediated CRISPR/Cas9 inactivation of control (WT) or AMPK α 1 and α 2 (DKO) in a pooled cell population plated into soft agar. 3 weeks later colony growth was visualized by photon flux.

(F) Annexin V staining in KP 368T1 AMPK DKO isogenic clones after treatment with 500 μ M phenformin or culture in low (2.5mM) or high (25mM) glucose for 48hrs (*left*), or culture in no (0mM) or high (25mM) glucose for 24hrs (*right*). % live cells (lower left quadrant) is shown below each plot.

(G) Cell cycle analysis of 368T1 AMPK DKO isogenic clones after culture in low (2.5mM) glucose for 12hrs. Data are represented as fold change relative to high glucose.

(H) Clonogenic growth of 634T isogenic clones in low glucose conditions (top) and quantitation (bottom).

(I) Cluster analysis of RNA-seq data of AMPK α 1 α 2 KO 368T1 cells with vector control (DKO) or AMPK α 1 (A1) stably reconstituted, and grown in high or no glucose conditions for 12 or 18 hours. Red box indicates AMPK-dependent genes.

(J-N) RNA-seq analysis of polyclonal KP 634T cells with CRISPR/Cas9-mediated deletion of AMPK α 1 and α 2 (AMPK KO) in the pooled cell population or control cells (WT) grown in high or no glucose conditions for 16 hours.

(J) Cluster analysis of RNA-sequencing data from AMPK α 1 α 2 KO 634T cells with control (WT) or AMPK α 1 α 2 KO (KO), and grown in no glucose conditions for 16 hours. R1 and R2 indicate different biological replicates. Red boxed regions include 486 genes which are upregulated in response to glucose deprivation in an AMPK-dependent manner.

(K) David Analysis of the genes within the red boxes in (J). All terms with Benjamini $<E^{-5}$ are shown.

(L) Genes within the red boxes in (J) were analyzed using Homer known motif enrichment analysis, considering -2000 to +500 around the TSS. The most significant term, TFE3, is shown.

(M) Gene set enrichment analysis (GSEA) plot from RNA-seq data in 16 hrs no glucose sorted by p-value, considering both biological replicates together. (NES) Normalized enrichment score; (FDR) false discovery rate.

(N) Western blot of AMPK KO (KO) or wildtype (WT) 634T cells treated with DMSO control (D) or 991 for 1hr, and high (HG) and low glucose (LG) for 24hrs.

All values are expressed as means \pm s.e.m. * $P<0.05$ ** $P<0.01$ *** $P<0.001$ relative to α 1 in B and D as determined by students t test.

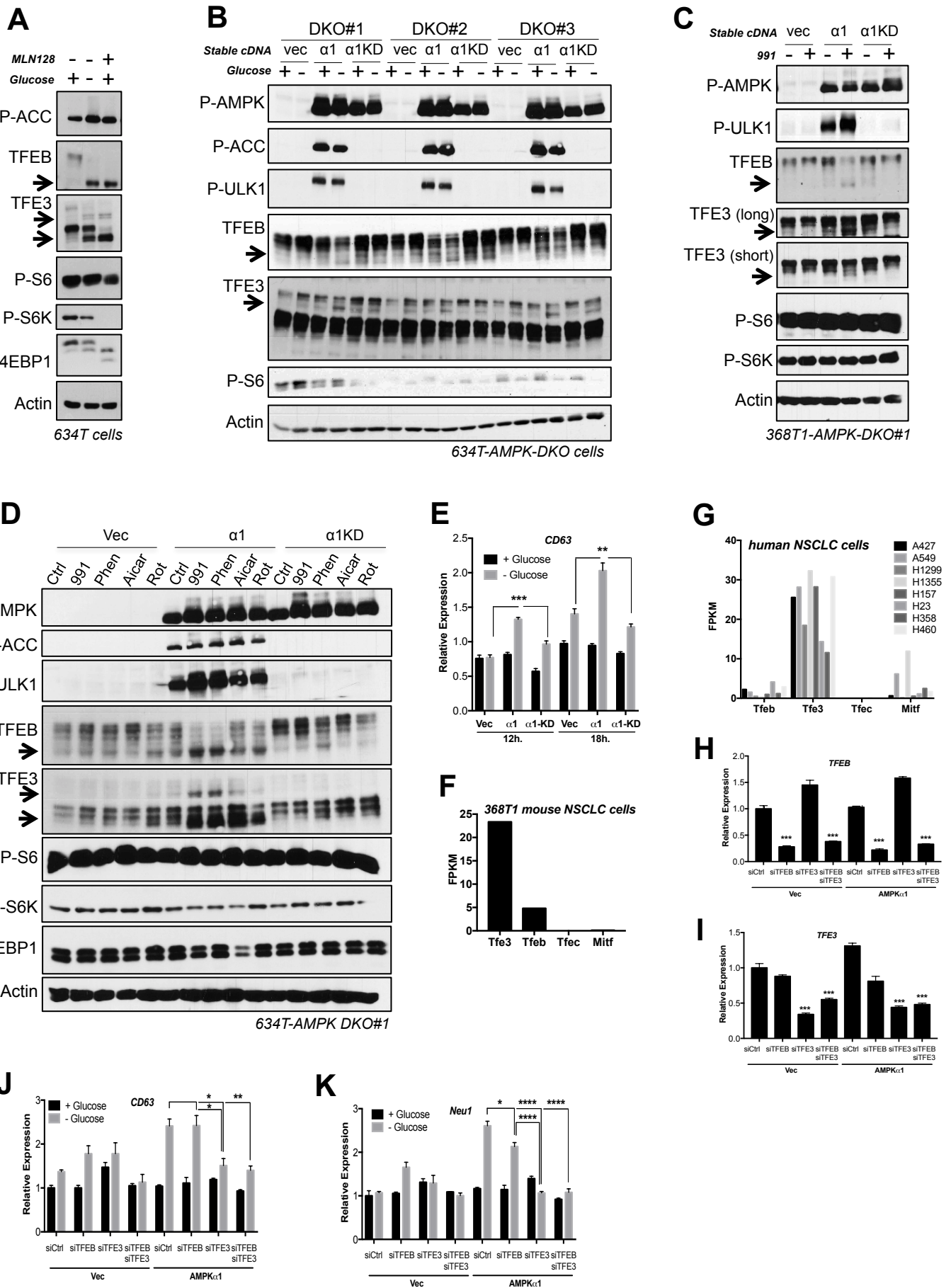


Figure S4

Figure S4: AMPK activation promotes de-phosphorylation, nuclear translocation and transcriptional activity of Tfeb and Tfe3, Related to Figure 4

(A) Western blot of 368T1 cells in the presence (+) or absence (-) of glucose, treated with 1 μ M MLN128 or non-treated for 6hrs. Arrows in blots highlight de-phosphorylated TFEB and TFE3.

(B) Western blot analysis of isogenic 634T AMPK knockout clones stably expressing either vector control (Vec), AMPK α 1 (α 1) or kinase-dead AMPK α 1 (α 1-KD) in the presence (+) or absence (-) of glucose (Gluc) for 12hrs. Arrows highlight de-phosphorylated Tfeb and Tfe3.

(C) Western analysis of 368T1-AMPK DKO#1 isogenic clones left untreated or treated with 991. Arrows highlight de-phosphorylated TFEB and TFE3.

(D) Western analysis of 634T-AMPK DKO#1 isogenic clones left untreated or treated with a panel of AMPK activating compounds. Arrows highlight de-phosphorylated TFEB and TFE3.

(E) qPCR for *CD63* expression in 368T1 isogenic clones cultured in the presence or absence of glucose for 12hrs or 18hrs.

(F) RNA expression levels (FPKM) of *Tfeb*, *Tfe3*, *Tfec* and *Mitf* in 368T1 cells.

(G) RNA expression levels (FPKM) of *Tfeb*, *Tfe3*, *Tfec* and *Mitf* in 8 human NSCLC cell lines.

(H-I) qPCR for *Tfeb* (H) and *Tfe3* (I) expression in 368T1-AMPK DKO vector or AMPK α 1 cells transfected with siRNAs targeting either control, *Tfeb*, *Tfe3* or *Tfeb* & *Tfe3*.

(J-K) qPCR for *CD63* (J) and *Neu1* (K) expression in 368T1 isogenic clones transfected with siRNAs targeting either control, *Tfeb*, *Tfe3* or *Tfeb* & *Tfe3* cultured in the presence or absence of glucose for 18hrs.

All values are expressed as means \pm s.e.m. * P<0.05 ** P<0.01 *** P<0.001 **** P<0.0001 determined by students t test or ANOVA with Tukeys method for multiple comparison.

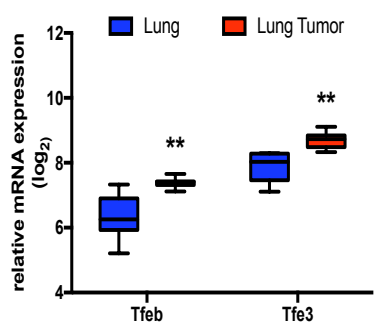
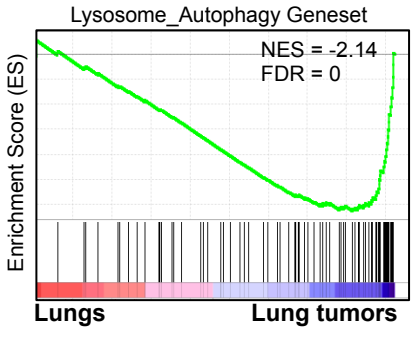
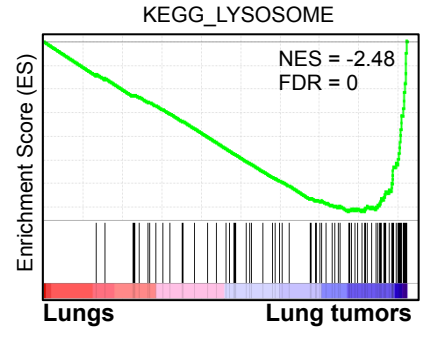
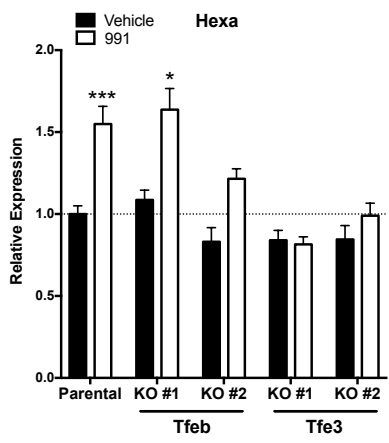
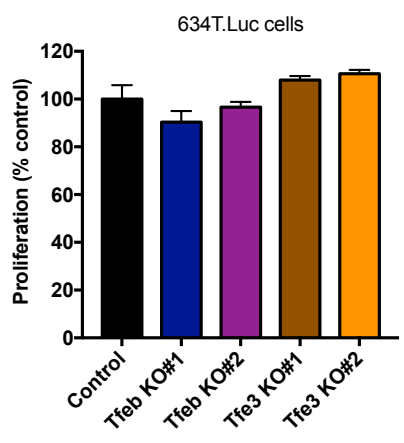
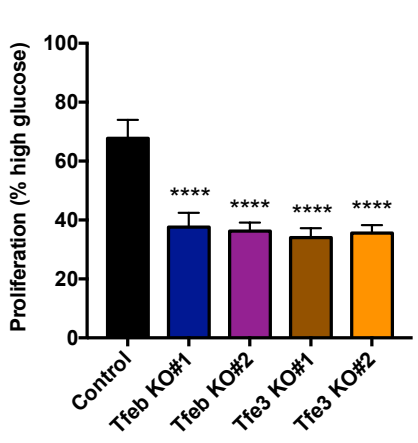
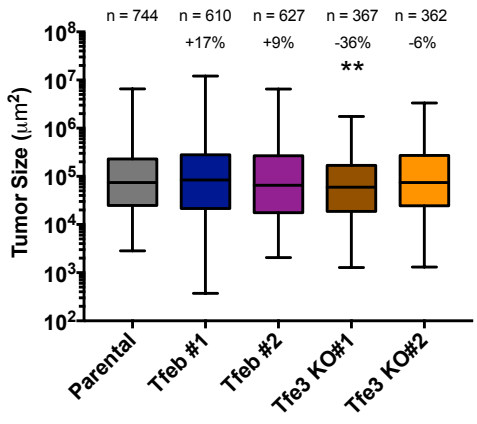
A(Sweet-Cordero et al, *Nature Genetics*, 2005)**B****C****D****E****F****G**

Figure S5: Tfe3 deletion impairs the growth of mouse NSCLC cells *in vivo*, Related to Figure 5

(A) mRNA expression levels of *Tfeb* and *Tfe3* from RNA-seq data from normal lung vs. *Kras*/+ lung tumors analyzed from Sweet-Cordero *et al*, *Nature Genetics*, 2005.

(B) GSEA plot for the Bardeesy lysosome-autophagy gene set (2016) in normal lung vs. *Kras*/+ lung tumors analyzed for the Sweet-Cordero *et al*, *Nature Genetics*, 2005 RNA-seq dataset.

(C) GSEA plot for the KEGG-lysosome gene set analyzed for the Sweet-Cordero *et al*, *Nature Genetics*, 2005 normal lung vs. *Kras*/+ lung tumors RNA-seq dataset.

(D) qPCR for *Hexa* expression in polyclonal 634T cell populations of CRISPR/Cas9-mediated deletion of *Tfeb* and *Tfe3* treated with 991 for 12hrs.

(E) Proliferation rates of 634T cells in high glucose after 48hrs. Data are represented as percent proliferation of parental control cells (control).

(F) Proliferation rates of 634T cells in low glucose after 48hrs. Data are represented as percent proliferation of cells in high glucose.

(G) Tumor size analysis. Number of tumors analyzed is indicated above each condition.

All values are expressed as means \pm s.e.m. * $P < 0.05$ ** $P < 0.01$ *** $P < 0.001$ **** $P < 0.0001$ determined by ANOVA with Tukeys method for multiple comparison.

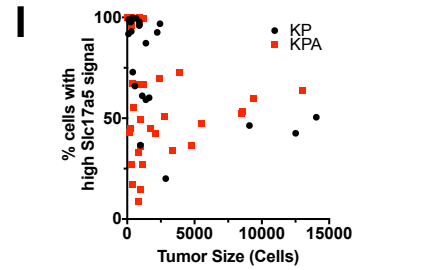
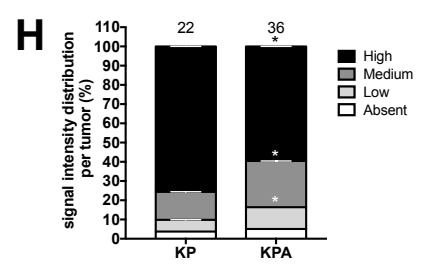
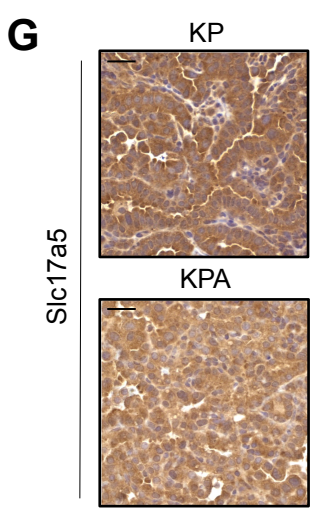
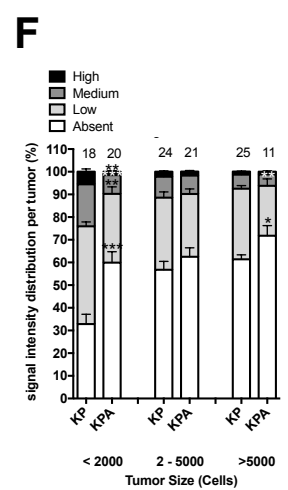
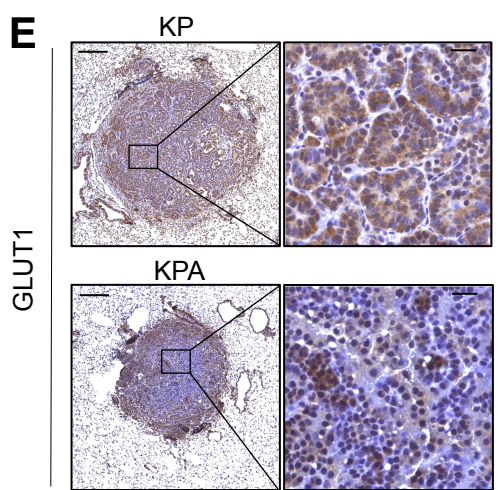
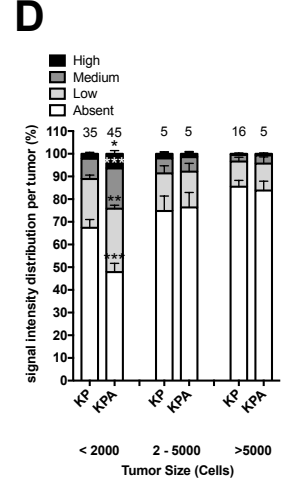
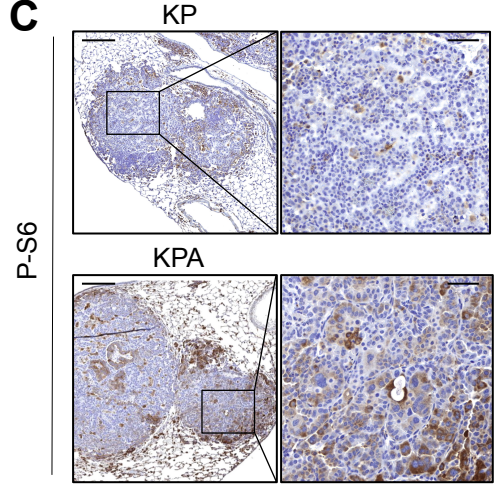
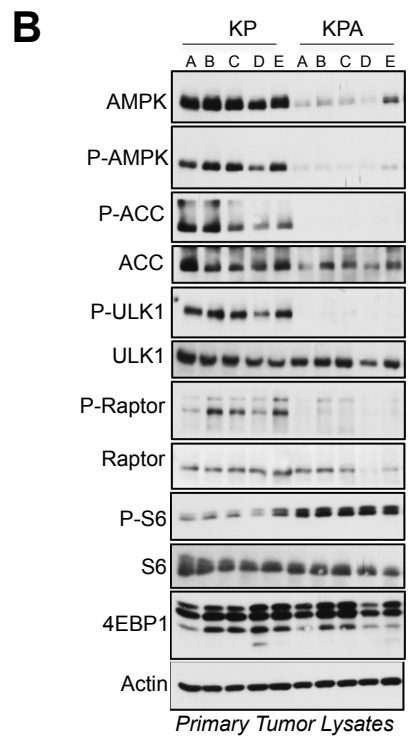
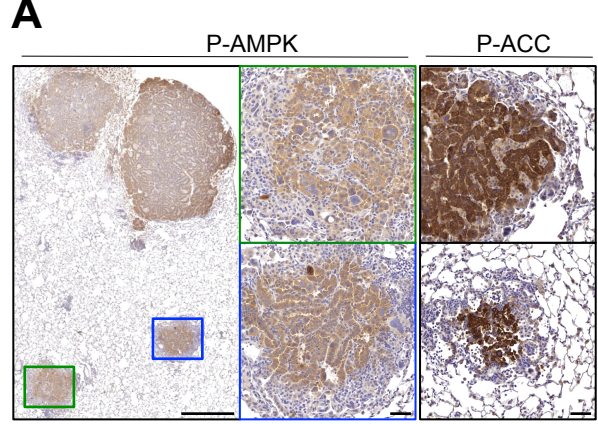


Figure S6

Figure S6: AMPK deletion impacts mTor signaling, Glut1 and the lysosomal pathway in KP lung tumors *in vivo*, Related to Figure 6

(A) Representative P-AMPK IHC image in KP tumors. Blue and green boxes are expanded to the right. Representative P-ACC IHC images from KP tumors with similar staining pattern as P-AMPK shown in right column. Scale bar, 500 μ m (left panel) and 50 μ m (right panels).

(B) Western blots on single primary tumor lysates from KP and KPA mice. Number of tumors analyzed per genotype is shown.

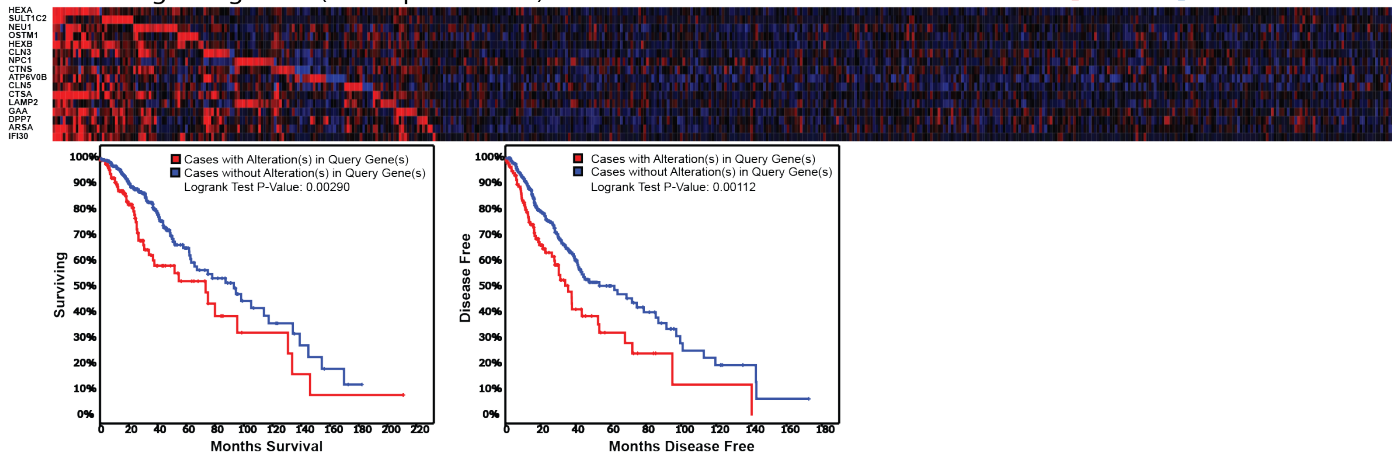
(C-D) Representative P-S6 IHC images (**C**) and quantitation of staining positivity per tumor binned by tumor size (**D**). Scale bar, 200 μ m (left) and 50 μ m (right).

(E-F) Representative Glut1 IHC images (**E**) and quantitation of staining positivity per tumor binned by tumor size (**F**). Scale bar, 200 μ m (left) and 20 μ m (right).

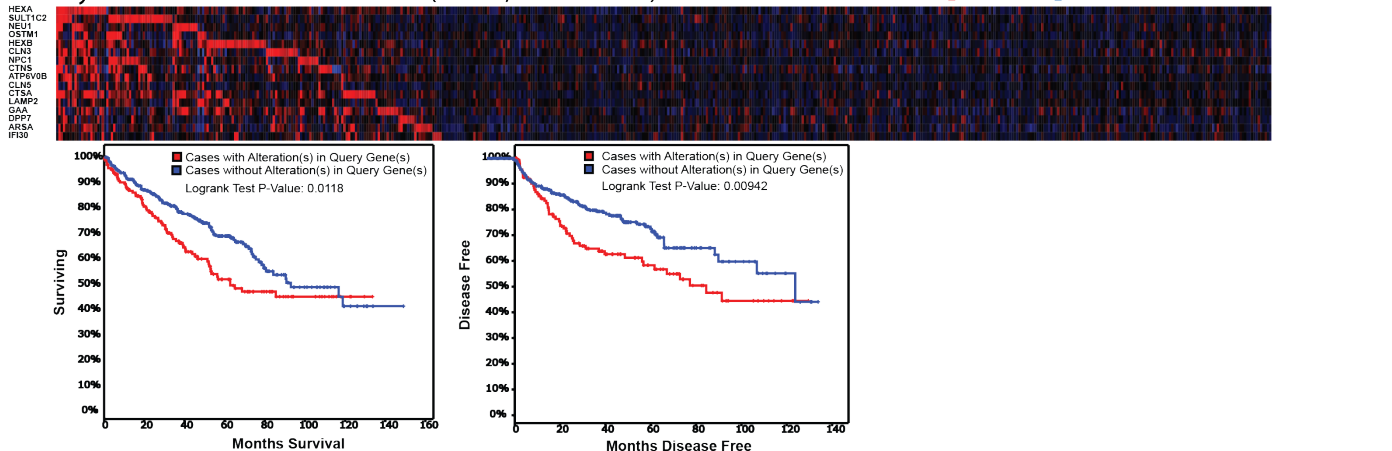
(G-I) Representative images from Slc17a5 IHC in KP and KPA tumors (**G**) and quantitation of staining intensity per tumor per genotype (**H**). (**I**) Tumors from (**H**) with High signal intensity plotted according to tumor size (cell number per tumor). Scale bar, 20 μ m.

IHC quantitation: number of tumors analyzed indicated above each column. All values are expressed as means \pm s.e.m. * P<0.05 ** P<0.01 *** P<0.001 determined by students t test or ANOVA with Tukeys method for multiple comparison.

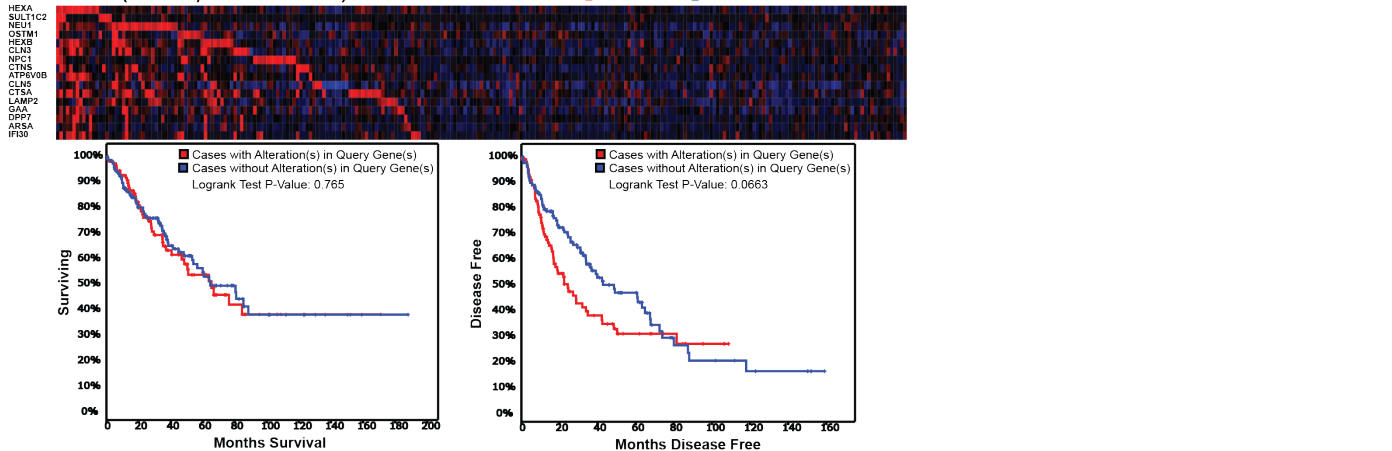
Brain lower grade glioma (TCGA provisional)



Kidney Renal Clear Cell Carcinoma (TCGA, Provisional)



Sarcoma (TCGA, Provisional)



Skin Cutaneous Melanoma (TCGA, Provisional)

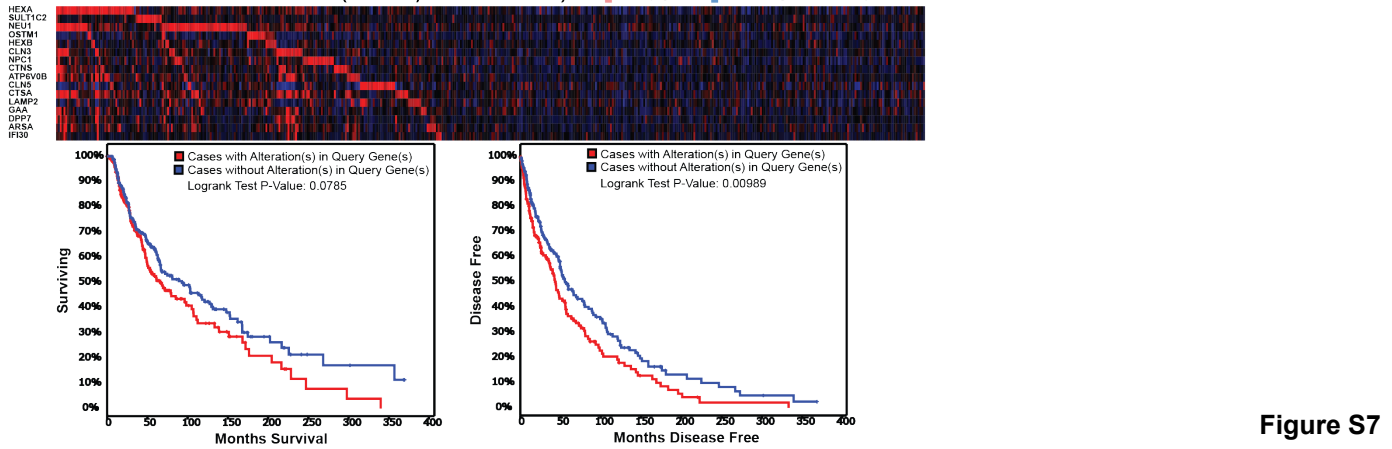


Figure S7

Figure S7: Elevated lysosomal gene expression correlates with accelerated disease recurrence and patient survival, Related to Figure 7

A stringent 16-gene AMPK-dependent lysosomal gene set was defined in Figure 3I and applied to stratify the TCGA Lung Adenocarcinoma dataset in Figure 7A. Our lysosomal gene set correlates with poor disease outcome as indicated by survival and disease free plots in 4 additional TCGA datasets, Brain lower grade glioma, Kidney renal clear cell carcinoma, Sarcoma, and Skin cutaneous melanoma. mRNA misregulation in at least one lysosomal gene set gene with an RNA-seq z-score cut-off set at +/- 2.0 is shown in the top panels. Patient samples were divided into two groups, those with modulation of mRNA levels of lysosomal gene set genes, "with alterations" (red), or those without major mRNA alterations in any of these genes, "without alterations" (blue).

Table S1. Additional Oligonucleotides, Related to STAR Methods

EXPERIMENT	NAME	SEQUENCE (5'-3')
CRISPR_sgRNA	mAMPKα1KO_1F	CACCG TATTGTCACAGGCATATGG
(bold = sequences added for cloning)	mAMPKα1KO_1 R	AAACCC ATATGCCTGTGACAATAAC
	mAMPKα2KO_1F	CACCG ACAGGCATATGGTTGTCCAT
	mAMPKα2KO_1 R	AAAC ATGGACAACCATATGCCTGTC
	mTfe3 gRNA #1-F	CACCG GAGGCGTGAGCGGCGGGAAC
	mTfe3 gRNA #1-R	AAAC GTTCCCGCCGCTCACGCCTCC
	mTfe3 gRNA #2-F	CACCG ATGGCTGGTGAGGCGGGCGC
	mTfe3 gRNA #2-R	AAAC GCGCCCGCCTCACCAGCCATC
	mTfeb gRNA #1-F	CACCG CAGCCCGATGCGTGACGCCA
	mTfeb gRNA #2-F	CACCG GCTGCCATGGCGTCACGCAT
	mTfeb gRNA #2-R	AAAC ATGCGTGACGCCATGGCAGCC
qPCR_mRNA	mTbp qPCR-F	CCTTGTACCCTTCACCAATGAC
	mTbp qPCR-R	ACAGCCAAGATTCACGGTAGA
	mTfeb qPCR-F	CGGACAGATTGACCTTCAGAG
	mTfeb qPCR-R	GCTGCTGCTGTTGCATATAAT
	mTfe3 qPCR-F	CGAGCCGTGTTCTGCTATT
	mTfe3 qPCR-R	TGCAGTGATATTGGGAGGCTG
	mHexa qPCR-F	TGGCCCCAGTACATCCAAAC
	mHexa qPCR-R	GGTTACGGTAGCGTCGAAAGG
	mCd63 qPCR-F	GAAGCAGGCCATTACCCATGA
	mCd63 qPCR-R	TGACTTCACCTGGTCTCTAAACA
	mNeu1 qPCR-F	GTAGACACTTTCCGCATCCC
	mNeu1 qPCR-R	CGATGAAGGCTGTAGAGGAC
	mAtp6v1d qPCR-F	TGCTGATGGGTGAAGTGATG
	mAtp6v1d qPCR-R	CAAACACTGGCAAGGTAACAC
	mSult1c2 qPCR-F	CCAACCATCAGGTGTGGACAA
	mSult1c2 qPCR-R	GGCTCATCCTGTAGAAGTGGT
	mAtp6v0b qPCR-F	CGGGATCTTTGTGGCCTTCT
	mAtp6v0b qPCR-R	GTTTCCGTCAGGAACCATGC